ACS Catalysis

pubs.acs.org/acscatalysis

Research Article

Scope and Mechanism of the Redox-Active 1,2-Benzoquinone Enabled Ruthenium-Catalyzed Deaminative α-Alkylation of Ketones with Amines

Pandula T. Kirinde Arachchige, Suhashini Handunneththige, Marat R. Talipov, Nishantha Kalutharage, and Chae S. Yi*

Cite This: *ACS Catal.* 2021, 11, 13962−13972

Read Online

ACCESS | Metrics & More | Article Recommendations | Supporting Information

ABSTRACT: The catalytic system formed *in situ* from the reaction of a cationic Ru−H complex with 3,4,5,6-tetrachloro-1,2-benzoquinone was found to mediate a regioselective deaminative coupling reaction of ketones with amines to form the α-alkylated ketone products. Both benzylic and aliphatic primary amines were found to be suitable substrates for the coupling reaction with ketones in forming the α-alkylated ketone products. The coupling reaction of $PhCOCD_3$ with 4-methoxybenzylamine showed an extensive H/D exchange on both α-CH_2 (41% D) and β-CH_2 (21%) positions on the alkylation product. The Hammett plot obtained from the reaction of acetophenone with *para*-substituted benzylamines *p*-X-$C_6H_4CH_2NH_2$ (X = OMe, Me, H, F, Cl, CF_3) showed a strong promotional effect by the amine substrates with electron-releasing groups ($\rho = -0.49 \pm 0.1$). The most significant carbon isotope effect was observed on the α-carbon of the alkylation product (C_α = 1.020) from the coupling reaction of acetophenone with 4-methoxybenzylamine. The kinetics of the alkylation reaction from an isolated imine substrate led to the empirical rate law: rate = *k*[Ru][imine]. A catalytically active Ru−catecholate complex was synthesized from the reaction of the cationic Ru−H complex with 3,5-di-*tert*-butyl-1,2-benzoquinone and PCy_3. The DFT computational study was performed on the alkylation reaction, which revealed a stepwise mechanism of the [1,3]-carbon migration step *via* the formation of a Ru(IV)-alkyl species with a moderate energy of activation ($\Delta G^{\ddagger}$ = 32−42 kcal/mol). A plausible mechanism of the catalytic alkylation reaction *via* an intramolecular [1,3]-alkyl migration of an Ru-enamine intermediate has been compiled on the basis of these experimental and computational data.

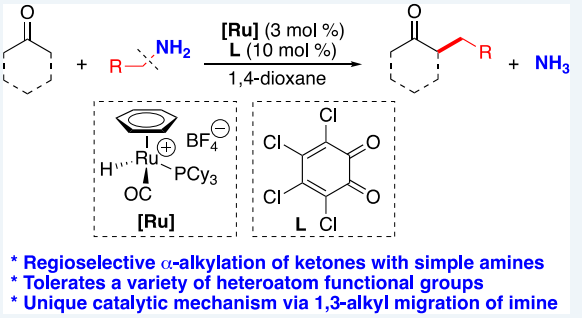

KEYWORDS: *alkylation, deaminative coupling, ruthenium catalyst, ketone, amine*

INTRODUCTION

The α-alkylation of carbonyl compounds *via* the generation of enolates represents one of the most widely used carbon−carbon bond formation methods in organic synthesis.[1] Because traditional alkylation methods using stoichiometric amounts of strong base and organic halide coupling partners lead to the formation of copious wasteful byproducts with a limited number of heteroatom functional group tolerance, concerted research efforts have been devoted to the development of selective catalytic alkylation protocols that would avoid the use of strong base and obviate the formation of wasteful byproducts. In particular, transition-metal-catalyzed "hydrogen borrowing" methodology, which involves the dehydrogenation of alcohols followed by aldol-type condensation with the ketone substrates, has been shown to be highly effective in promoting the alkylation of ketones with alcohols.[2] In a significant advancement for sustainable synthesis, earth-abundant transition-metal catalysts have been successfully employed for the catalytic alkylation method by using hydrogen-borrowing technology.[3] A number of novel catalytic C−H functionalization methods have been devised to promote direct alkylation and alkenylation of ketones with alkenes and alkynes.[4] In a seminal report, MacMillan and co-workers developed a direct β-arylation of cyclic ketones with electron-deficient aryl nitriles by combining photocatalysis with an organocatalytic enamine alkylation protocol.[5] Fagnoni and co-workers employed photoactive tungsten catalysts to achieve the direct coupling of cyclopentanones with electron-deficient alkenes to give β-alkylated products.[6] Widenhoefer and Che groups independently reported intramolecular C−H alkylation methods for γ,σ-enone substrates to form cyclic ketones by using Pd and Au

Received: October 13, 2021

https://doi.org/10.1021/acscatal.1c04732
ACS Catal. 2021, 11, 13962−13972

catalysis.[7] Dong and co-workers recently reported a direct α-alkylation of ketones with simple alkenes by using a bifunctional Rh catalytic system, in which an *aza*-indoline moiety was found to promote the conversion of the α-C−H bond of ketones into an enamine sp^2 C−H bond prior to the alkylation reaction.[8]

In recent years, transition-metal-catalyzed deaminative coupling methods have emerged as an effective tool for promoting a variety of C−C bond coupling reactions.[9] Glorius and co-workers devised an efficient deaminative alkylation of amines *via* the generation of pyridinium ions by employing visible-light photoredox catalysis.[10] The Zhang group reported Pd-catalyzed allylic alkylation of carbonyl compounds with allylamines, which has been shown to involve a direct allylic C−N bond cleavage *via* the formation of Pd-allyl species.[11] Martin and co-workers recently reported a highly regioselective Ni-catalyzed deaminative alkylation of unactivated olefins by using pyridinium reagents.[12] Fu and co-workers reported an efficient photocatalytic deaminative and decarboxylative alkylation of silyl enol ethers with redox-active esters and *N*-alkylpyridinium salts.[13] From both synthetic and environmental points of view, catalytic C−C coupling methods *via* C−N cleavage by employing readily available amines as the substrates have been regarded as a highly attractive strategy for the synthesis of complex organic molecules as well as for reforming processes of nitrogen-containing biomass feedstocks.[9,14]

We previously discovered that the cationic ruthenium hydride complex $[(\eta^6\text{-}C_6H_6)(PCy_3)(CO)RuH]^+BF_4^-$ (**1**) is a highly effective catalyst precursor for the deaminative and decarboxylative coupling reaction of ketones with amino acids.[15] We subsequently found that the ruthenium−hydride complex **1** with a 1,2-catechol ligand exhibits an exceptionally high chemoselectivity for promoting the deaminative coupling reactions of amines to form unsymmetric secondary amines and quinazolinone derivatives.[16] To extend the synthetic utility of ligand-controlled catalysis, we have been exploring the promotional effects of various oxygen and nitrogen donor ligands on ruthenium catalysts for the deaminative coupling reactions of amines. Herein, we report the development and scope of a highly regioselective catalytic deaminative α-alkylation method of ketones with amines, which is mediated by a well-defined ruthenium catalyst containing a redox-active *ortho*-benzoquinone ligand. We also delineate comprehensive experimental and computational studies for establishing a detailed mechanism of the catalytic alkylation reaction. The salient features of the catalytic method are that the α-alkylation ketone products are formed in regio- and stereoselective fashions without employing any reactive reagents or forming any wasteful byproducts, while tolerating a number of common organic functional groups.

RESULTS AND DISCUSSION

Reaction Scope. We recently found that cationic Ru−H complex **1** with a 1,2-catechol ligand is an effective catalytic system for promoting the deaminative coupling of amines to form unsymmetric secondary amines.[16] While searching for a suitable catalytic system for the deaminative coupling reactions, we initially discovered that the catalytic system consisted of Ru−H complex **1** and a redox-active 1,2-benzoquinone ligand exhibited high catalytic activity for the deaminative coupling of acetophenone with 4-methoxybenzylamine to form α-alkylation product **2a** (eq 1). The addition of a 1,2-benzoquinone ligand was found to substantially enhance the catalytic activity of **1**, as the Ru catalyst without the ligand yielded a low product yield (Table 1). The Ru−H complex **1** with 3,4,5,6-tetrachloro-1,2-benzoquinone (**L1**) was found to exhibit the highest activity among screened ruthenium catalysts and benzoquinone ligands, where 1,4-dioxane was found to be the most suitable solvent for the coupling reaction. Subsequent ligand screening and optimization efforts have led to the standard conditions for the coupling reaction: acetophenone (0.50 mmol), benzylamine (0.70 mmol), **1** (3 mol %), and **L1** (10 mol %) in 1,4-dioxane (2 mL) at 130 °C for 16 h (Table S1, Supporting Information). The ammonia byproduct, which was detected by GC−MS in a crude reaction mixture, was removed under vacuum along with the solvent, and product **2a** was isolated by a column chromatographic separation on silica gel.

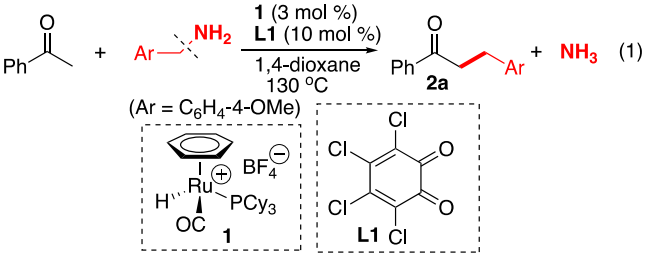

Table 1. Catalyst and Additive Screening for the Coupling of Acetophenone with 4-Methoxybenzylamine[a]

entry	catalyst	deviation from standard conditions	**2a** (%)[b]
1	**1**	none	92
2	**1**	no **L1**	28
4	**1**	with **L3**[c]	64
3	**1**	with **L13**[c]	78
5	**1**	at 100 °C	trace
6	$[(PCy_3)_2(CO)(CH_3CN)_2RuH]BF_4$		56
7	$[(PCy_3)(CO)RuH]_4(O)(OH)_2$	with $HBF_4{\cdot}OEt_2$	79
8	$(PCy_3)_2(CO)RuHCl$		22
9	$RuCl_2(PPh_3)_3$		16
10	$Ru_3(CO)_{12}/HBF_4{\cdot}OEt_2$		trace
11	$[(COD)RuCl_2]_x/HBF_4{\cdot}OEt_2$		trace
12	$PCy_3/HBF_4{\cdot}OEt_2$		0
13	$BF_3{\cdot}OEt_2$		0
14	$HBF_4{\cdot}OEt_2$		0
15		without **1**	0

[a]Standard conditions: acetophenone (0.50 mmol), 4-methoxybenzylamine (0.70 mmol), **1** (3 mol %), **L1** (10 mol %), 1,4-dioxane (2 mL), 130 °C, 16 h. [b]The product yield of **2a** was determined by ^{1}H NMR using hexamethylbenzene as an internal standard. [c]**L3** = 3,5-*bis*(1,1-dimethylethyl)-3,5-cyclohexadiene-1,2-dione, **L13** = 3,5-*bis*(1,1-dimethylethyl)-1,2-benzenediol. See Table S1 (Supporting Information) for the complete list of screened ligands.

The substrate scope of the deaminative alkylation reaction was explored by using the *in situ* generated catalyst system **1**/**L1** under the standard conditions (Table 2). Both benzylic and aliphatic primary amines were found to be suitable substrates for aryl-substituted ketones to form the α-alkylation products **2a**−**m**. The analogous coupling of aliphatic ketones with benzylic and aliphatic amines cleanly formed the α-alkylated ketone products **2n**−**t**. The coupling reaction of the substituted cyclic ketones with benzylic amines resulted in a highly diastereoselective alkylation products **2u**−**w**. In contrast, the coupling of cyclohexanone with a chiral amine (*R*)-(+)-β-methylphenethylamine resulted in a 2.8:1 diastereomeric mixture of **2aa**. In general, the alkylation occurs regioselectively at the less

https://doi.org/10.1021/acscatal.1c04732
ACS Catal. 2021, 11, 13962−13972

Table 2. Deaminative α-Alkylation of Ketones with Amines[a]

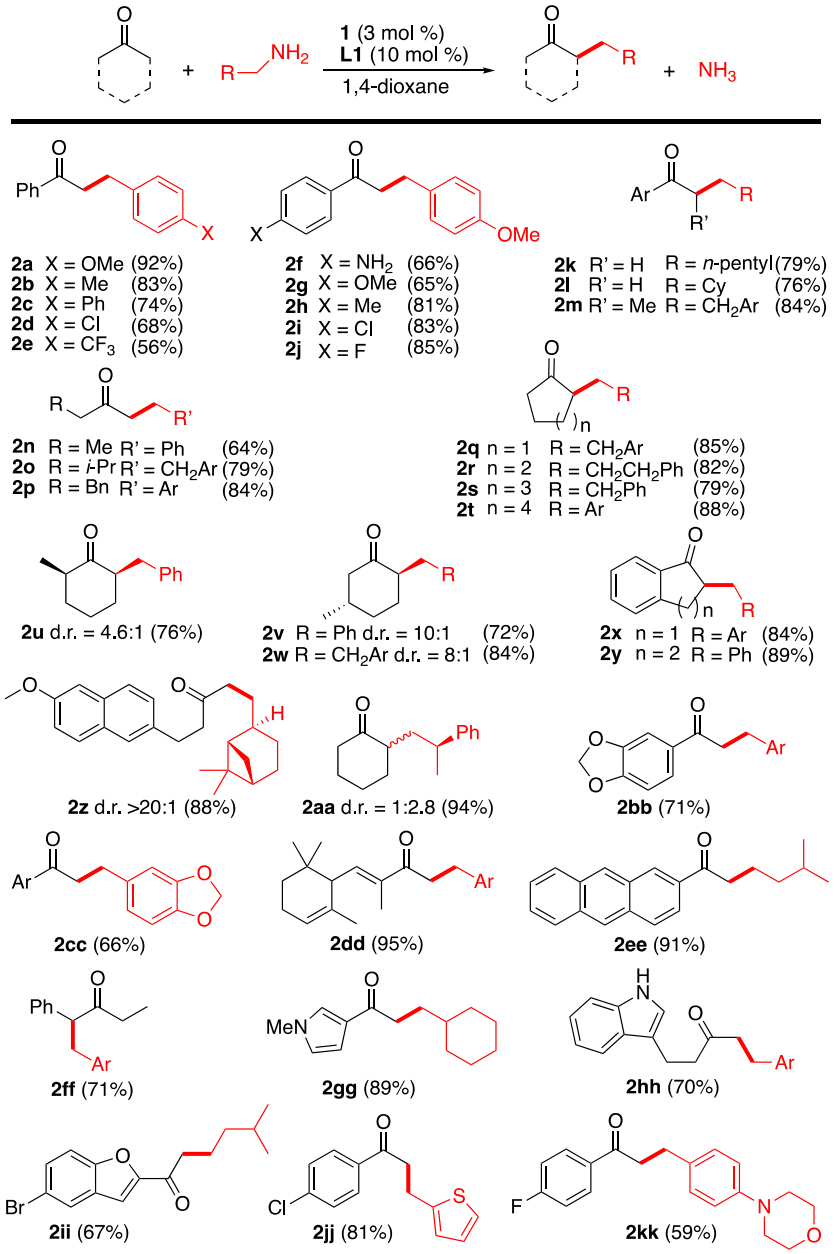

[a]Reaction conditions: ketone (0.5 mmol), amine (0.7 mmol), **1** (3 mol %), **L1** (10 mol %), 1,4-dioxane (2 mL), 130 °C, 16 h. Ar = 4-methoxyphenyl.

substituted α-carbon of ketones, but the coupling of 1-phenyl-2-butanone with a benzylic amine formed the branched alkylated product **2ff**, resulting from the regioselective alkylation on the phenyl-substituted carbon. Nitrogen-containing ketones smoothly formed the coupling products, as illustrated by the formation of **2gg**,**hh**, and thiophene- and morpholine-substituted benzylamines yielded the alkylation products **2jj** and **2kk**, respectively. Sterically demanding primary amines or secondary amines with α-quaternary carbon did not give any alkylation products.

We next surveyed the substrate scope of the coupling method by employing a number of biologically active ketone and amine substrates to further demonstrate its synthetic utility (Table 3). The coupling of an indole-substituted ketone with (−)-*cis*-myrtanylamine yielded coupling product **2ll** without any detectable racemization on the chiral methyne position, the structure of which was determined by X-ray crystallography. The treatment of nabumetone with geranylamine led to coupling product **2mm**, with the regioselective hydrogenation on the proximal double bond. The treatment of 4-morpholinylacetophenone with 4-methoxybenzylamine cleanly afforded α-alkylated product **2nn**, the structure of which was also confirmed by X-ray crystallography. The coupling of acetone with (+)-dehydroabietylamine led to an essentially single diastereomer of alkylation product **2qq**, while the coupling of 5-α-cholestan-3-one with *iso*-amylamine resulted in a 6:1 diastereomeric mixture of product **2rr**. These examples amply illustrate the synthetic utility as well as heteroatom functional group compatibility of the catalytic method in forming α-alkylated ketone products.

https://doi.org/10.1021/acscatal.1c04732
ACS Catal. 2021, 11, 13962−13972

Table 3. Deaminative α-Alkylation of Ketones with Biologically Active Amines[a]

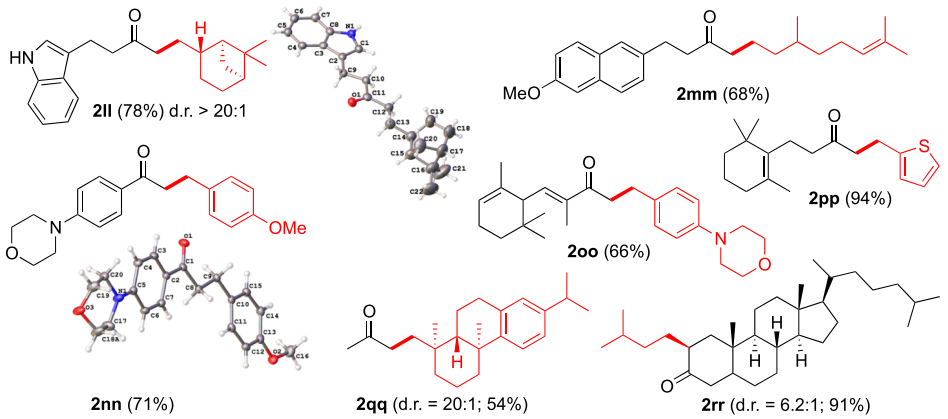

[a]Reaction conditions: ketone (0.50 mmol), amine (0.70 mmol), **1** (3 mol %), **L1** (10 mol %), 1,4-dioxane (2 mL), 130 °C, 16−20 h.

Reaction Profile and Crossover Experiment. We have chosen the reaction of acetophenone with benzylic amines for probing the mechanism of alkylation reaction. First, we monitored the coupling reaction of acetophenone with 4-methoxybenzylamine by NMR in an effort to profile the catalytic reaction. Thus, the treatment of acetophenone (0.10 mmol) with 4-methoxybenzylamine (0.10 mmol) in the presence of complex **1** (3 mol %)/**L1** (10 mol %) in toluene-d_8 (0.5 mL) in a J-Young NMR tube was immersed in an oil bath set at 130 °C. The tube was taken out from the oil bath in 20 min intervals and was analyzed by ^{1}H NMR at ambient temperature. As shown in Figure 1, a rapid formation of the imine product PhMeC═$NCH_2C_6H_4$-4-OMe (**3a**) was initially observed, reaching at its maximum concentration within 40 min. After 1 h, alkylation product **2a** was gradually appeared at the expense of **3a**, and the complete conversion to **2a** took about 3 h of the reaction time under these conditions. The formation of **2a** was found to exhibit the first-order kinetics, as indicated by a linear plot of *ln*[**2a**] *versus* time (*vide infra*).

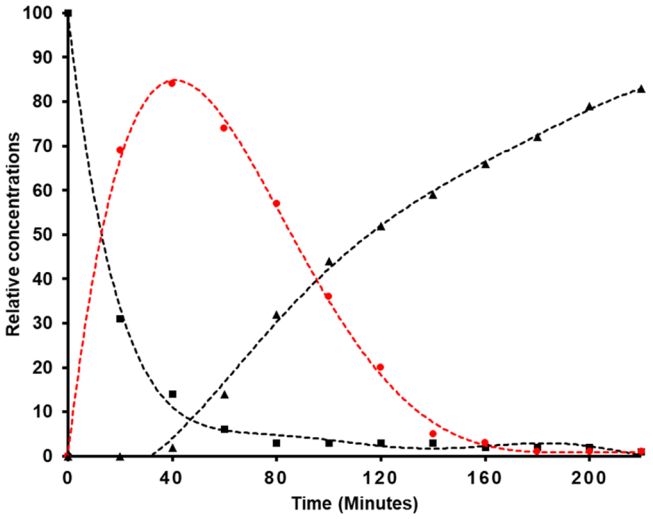

Figure 1. Reaction profile for the coupling reaction of acetophenone with 4-methoxybenzylamine. Acetophenone (■), **2a** (▲), and **3a** (red ●).

In a separate preparatory-scale experiment, we have been able to isolate the imine product **3a** in 99% yield from the dehydrative coupling reaction of acetophenone with 4-methoxybenzylamine. The subsequent treatment of isolated imine **3a** with **1** (3 mol %)/**L1** (10 mol %) and water (2 equiv) under the standard conditions cleanly formed product **2a** in >95% yield (eq 2). In this case, the addition of water was found to be essential because a stoichiometric amount of water is necessary for the hydrolysis of imine in forming ketone product **2a**.

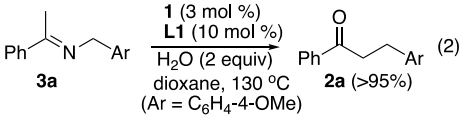

Both the reaction profile and the imine reaction experiments established that imine **3a** is the requisite intermediate for alkylation product **2a**. To probe whether **2a** is resulted from an intramolecular or an intermolecular disproportionation process, we next performed a set of crossover experiments by using the preformed imine substrates. Thus, a 1:1 mixture of the independently generated **3a** (0.25 mmol) and *N*-cyclohexylidene-3-phenylpropan-1-amine (**3b**) (0.25 mmol) in 1,4-dioxane (2 mL) was treated with the catalytic system **1**/**L1** and water (0.50 mmol) for 16 h under otherwise the standard reaction conditions (eq 3). The isolated product mixture contained a nearly 1:1 mixture of products **2a** and **2r** in 94 and 85%, respectively, with only a small amount of the crossover products (<10%). The absence of crossover coupling products indicates that the conversion of initially formed Schiff base **3** to alkylation product **2** predominantly proceeds *via* an intramolecular process.

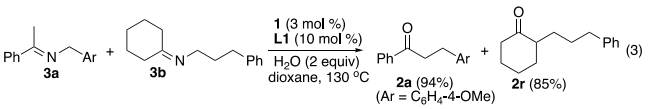

Deuterium Labeling Study. We next examined the deuterium exchange pattern of the coupling reaction to probe a possible imine-to-enamine isomerization process. Thus, the treatment of perdeuterated acetophenone $C_6D_5COCD_3$ (0.50 mmol) with 4-methoxybenzylamine (0.70 mmol) in the presence of **1** (3 mol %)/**L1** (10 mol %) under the standard conditions formed the coupling product **2a**-*d*, which was isolated by column chromatography on silica gel (eq 4). The

https://doi.org/10.1021/acscatal.1c04732
ACS Catal. 2021, 11, 13962−13972

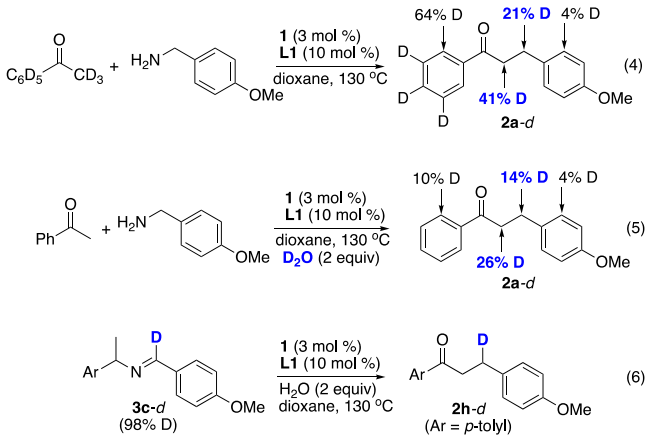

deuterium content of isolated product **2a**-*d* showed 41% on α-CH_2 and 21% on β-CH_2 positions as analyzed by ^1H and ^2H NMR (Figure S2, Supporting Information). The analogous coupling reaction of acetophenone with 4-methoxybenzylamine and D_2O (2 equiv) resulted in 26% deuterium incorporation on the α-CH_2 and 14% on the β-CH_2 positions of the product **2a**-*d* (eq 5). In a control experiment, the treatment of **2a** with D_2O (2 equiv) under the standard conditions led to the significant deuterium exchange only to the α-CH_2 (30% D) without any measurable deuterium on β-CH_2 position of product **2a**.

A relatively high degree of H/D exchange on the α-CH_2 group of the isolated product **2a**-*d* suggests a facile keto−enol tautomerization of the ketone product during and after the coupling reaction. In contrast, a significant amount of deuterium incorporation (21% D) on the β-CH_2 position of the product **2a**-*d* supports the notion that the H/D exchange resulted from the coupling reaction with the amine substrate, as noted by the absence of deuterium exchange under the control experiment conditions. The H/D exchange to α-CH_2 position can be readily explained by a facile and reversible imine−enamine tautomerization process, while the exchange to the β-CH_2 position can be explained *via* an initial amine-imine dehydrogenation reaction (Scheme S1, Supporting Information). However, an alternate mechanism *via* the carbonyl-assisted 5-membered metallacyclic species cannot be ruled out at this point, in light of the recent development of carbonyl-directed catalytic sp^3 C−H functionalization methods.[17] In an unrelated process, an extensive H/D exchange on the *ortho*-arene position (64% of D) can be explained *via* the chelate-assisted *ortho*-metalation and the reversible H/D exchange because such an *ortho*-arene C−H/C−D exchange pattern has been commonly observed for chelate-assisted arene C−H insertion reactions.[18]

To probe reversible H/D exchange during the imine−enamine tautomerization process, we prepared a deuterium-labeled imine substrate **3c**-*d* from the reaction of 4-methoxybenzaldehyde-d_1 with 1-*p*-tolylethanamine. The treatment of **3c**-*d* (98% D) with H_2O (2 equiv) under the standard conditions led to the formation of **2h**-*d* with the exclusive deuterium on the β-CH_2 position (49% D), which amounts to >98% retention of the deuterium atom (eq 6). The absence of significant H/D exchange in the formation **2h**-*d* is consistent with an irreversible C═N isomerization of an aldimine **3c**-*d* to a more stable ketimine prior to the product formation. A similar imine−enamine tautomerization process has been exploited in a number of metal-catalyzed C−C and C−N coupling reactions.[19]

Hammett Study. To probe electronic effects for the alkylation reaction, we compared the rates of the alkylation reaction of acetophenone with a series of *para*-substituted benzylamines *p*-X-$C_6H_4CH_2NH_2$ (X = OMe, Me, H, F, Cl, CF_3) (eq 8). The rate of the coupling reaction of acetophenone (0.20

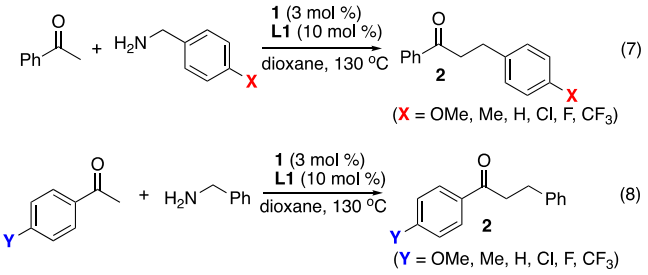

mmol) with a *para*-substituted benzylamine (0.30 mmol) in the presence of **1** (3 mol %)/**L1** (10 mol %) in toluene-d_8 was monitored by NMR. The appearance of product peak **2** was normalized against an internal standard (C_6Me_6) in 30 min intervals, and the k_{obs} of each catalytic reaction was determined from a first-order plot of $ln[([\mathbf{2}]_i - [\mathbf{2}]_t)/([\mathbf{2}]_i)_0]$ *versus* time. The Hammett plot of $\log(k_X/k_H)$ *versus* σ_p showed a linear correlation, in which the reaction is strongly promoted by an electron-releasing group of the amine substrate ($\rho = -0.49 \pm 0.1$) (Figure 2).

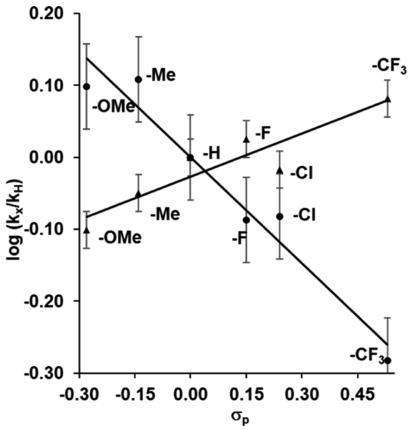

Figure 2. Hammett plots from the reaction of acetophenone with *p*-X-$C_6H_4CH_2NH_2$ (X = OMe, Me, H, F, Cl, CF_3) (●) and from the reaction of *p*-Y-$C_6H_4COCH_3$ (Y = OMe, Me, H, F, Cl, CF_3) with 4-methoxybenzylamine (▲).

The analogous Hammett plot was also obtained from the alkylation reaction of a series of *para*-substituted acetophenones *p*-Y-C_6H_4COMe (Y = OMe, Me, H, F, Cl, CF_3) with 4-methoxybenzylamine (eq 7). The rate of the coupling reaction of a *para*-substituted acetophenone (0.20 mmol) with 4-methoxybenzylamine (0.30 mmol) in the presence of **1** (3 mol %)/**L1** (10 mol %) in toluene-d_8 was measured by NMR, and the k_{obs} of each catalytic reaction was determined from a first-order plot of $ln[([\mathbf{2}]_i - [\mathbf{2}]_t)/([\mathbf{2}]_i)_0]$ *versus* time. In this case, the coupling reaction was moderately promoted by an electron-withdrawing group of the ketone substrate, as indicated by a relatively modest slope ($\rho = +0.20 \pm 0.1$). The pronounced promotional effect from the *para*-electron-releasing group of benzylamines suggests that the C−N bond cleavage step is strongly influenced by the nucleophilicity of the benzylic carbon. On the other hand, a moderate promotional effect from electron-deficient *para*-substituted acetophenones indicates that the electrophilic nature of the α-carbon of the ketone

https://doi.org/10.1021/acscatal.1c04732
ACS Catal. 2021, 11, 13962−13972

substrate is a significant factor for the C−C bond formation step.[20]

Carbon Isotope Effect Study. The Hammett study implicates that either C−N bond cleavage or C−C bond formation is most likely the rate-limiting step for the catalytic reaction. In an effort to discern between these possible turnover limiting steps, we measured a carbon kinetic isotope effect for the coupling reaction by employing Singleton's NMR technique at natural abundance.[21] Thus, the treatment of acetophenone (2.0 mmol) with 4-methoxybenzylamine (2.8 mmol) in the presence of **1** (3 mol %)/**L1** (10 mol %) in 1,4-dioxane (8 mL) was heated at 130 °C for 20 h (eq 9). The product **2a** was

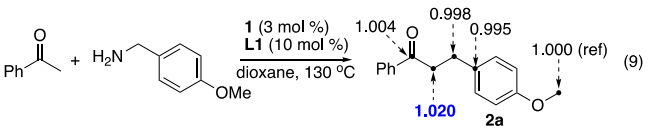

isolated by a column chromatography on silica gel, and the procedure was repeated three times to obtain a high conversion product sample of **2a**. The same experimental procedure was used for the isolation of a low conversion product sample of **2a**. High-precision ^{13}C NMR analysis showed a significant carbon isotope effect on the α-carbon of the product **2a** when the ^{13}C ratio of the product from a high conversion was compared with the sample obtained from a low conversion [^{13}C (avg 77% conversion)/^{13}C (avg 13% conversion) at C_α = 1.020; average of three runs] (Table S3, Supporting Information). The observed carbon isotope effect on the α-carbon of product **2a** can be rationalized *via* an asynchronous transition state on the C−C bond formation step. In support of this notion, Singleton and co-workers showed that the observation of most pronounced carbon isotope effect is definitive evidence for establishing the rate-limiting step for both C−C and C−O bond-forming reactions.[22] The C−N bond cleavage step has also been commonly considered as the turnover limiting step for catalytic reductive coupling reactions of amines and related organo-nitrogen compounds.[14]

Empirical Rate Law. We measured kinetics of the alkylation reaction as a function of [**1**], [**3a**], and [H_2O] under the conditions illustrated in eq 2. We used the isolated imine **3a** as the substrate to avoid induction period kinetics during the formation of **3a** and possible accumulation of intermediate species from the initial dehydration reaction. The initial rate was measured from the appearance of the product of **2a** at four different catalyst concentrations (4−20 μM). The plot of the initial rate (ν_0) as a function of [**1**] yielded a linear slope with the first-order rate constant of 2.8 × 10^{-3} s^{-1} (Figure 3A). The measurement of the initial rate as a function of the substrate concentration [**3a**] (0.2−0.8 mM) also showed the first-order rate dependence on **3a** in the range of the catalytically relevant concentrations (0.2−0.8 m*M*) (Figure 3B). On the other hand, the plot of initial rate *versus* [H_2O] showed a zero-order dependence in the range of 0.4−1.2 mM (Figure 3C). On the basis of these kinetic data, the empirical rate law for the reaction has been compiled as: rate = k[**1**][**3a**]. The first-order rate dependence on both [**3a**] and the catalyst [**1**] is consistent with an intramolecular process on the formation of **2a**, whereas the rate independence on [H_2O] indicates a facile imine hydrolysis step during the catalysis.

Synthesis and Catalytic Activity of the Ru−Catecholate Complex. In an effort to detect/trap catalytically relevant species, we examined the reaction of **1** with a number of catechol and benzoquinone ligands. Thus, the treatment of **1** (0.20 mmol) with 3,5-di-*tert*-butyl-1,2-benzoquinone (**L3**) (0.20 mmol) and PCy_3 (0.20 mol) in CH_2Cl_2 (3 mL) at 70 °C cleanly formed the Ru-catecholate complex **4**, which was isolated in 56% yield after recrystallization in a pentane/acetone solution (eq 10).[23] The molecular structure of complex **4** as

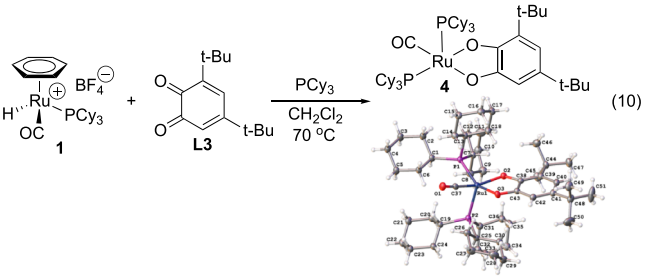

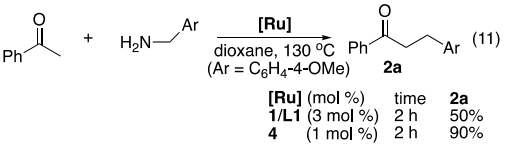

determined by X-ray crystallography showed a distorted square pyramidal geometry with two PCy_3 ligands occupying in apical and equatorial positions (∠ P−Ru−P = 112.3°).

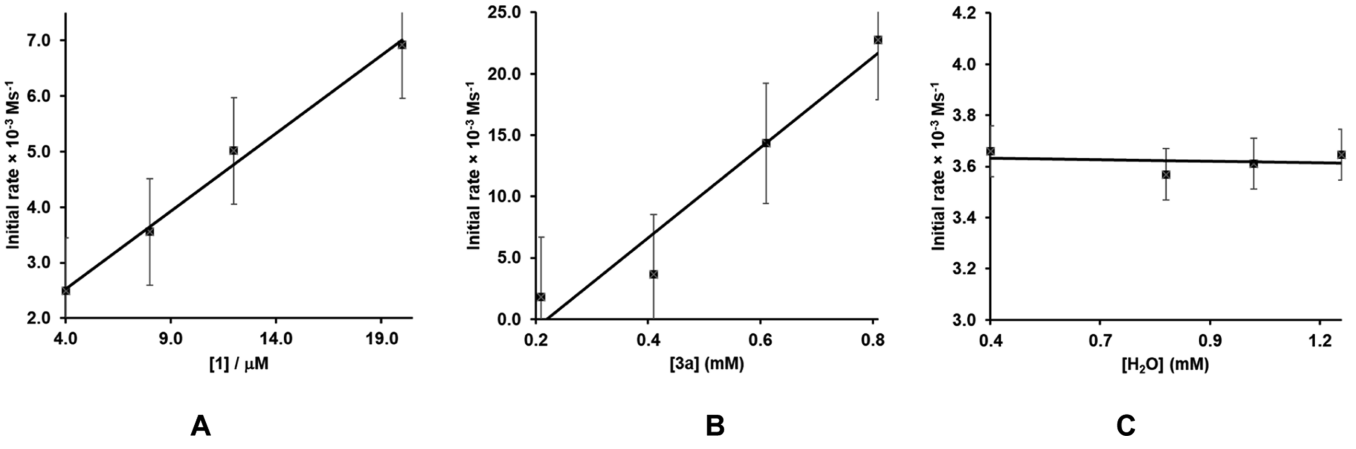

Figure 3. Plots for the initial rate *vs* [**1**] (A), *vs* [**3a**] (B), and *vs* [H_2O] (C).

https://doi.org/10.1021/acscatal.1c04732
ACS Catal. 2021, 11, 13962−13972

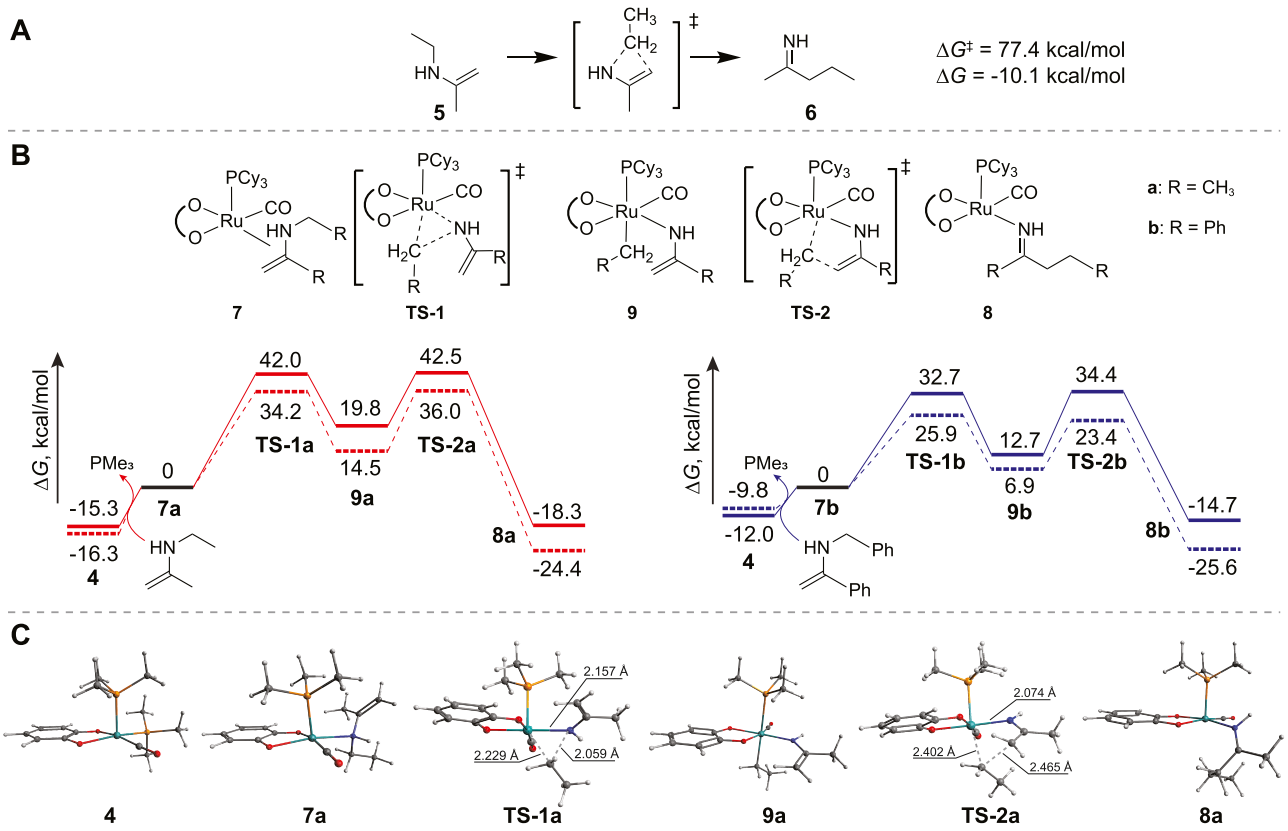

Figure 4. (A) Schematic representation of a sigmatropic transformation of *N*,*N*-ethyl-2-propenylamine into pentan-2-imine without a Ru catalyst. (B) Free energy profile for the alkylation reaction of **7a** to **8a** (red line) and **7b** to **8b** (blue line). Solid lines represent the free energy profile calculated at the M06L/def2-TZVPPD//M06L/def2-SV(P)+PCM(1,4-dioxane) level of theory (see the Supporting Information for computational details), and dash lines show similar calculations at the BP86/def2-TZVPPD//BP86/def2-SV(P)+PCM(1,4-dioxane) level. (C) Equilibrium geometries corresponding to the reaction profile shown in Figure B (left) obtained using the M06L functional basis set.

Complex **4** was found to exhibit a high catalytic activity for the alkylation reaction. For example, the treatment of acetophenone with 4-methoxybenzylamine in the presence of **4** (1 mol %) otherwise under the standard conditions efficiently afforded the alkylation product **2a** in 90% yield within 2 h (eq 11). We noted that the catalytic activity of **4** is substantially higher than the *in situ* generated one, giving the desired product **2a** in a shorter reaction time at a lower catalyst loading. We quantitatively measured the rate of the transformation of imine **3a** into **2a** by using the catalyst **4** under the similar conditions, as described in Figure 3. The initial rate of the appearance of the product **2a** was measured at four different catalyst concentrations (4−12 μM), and the plot of the initial rate (ν_0) as a function of [**4**] yielded the observed rate constant $k = 7.0 \times 10^{-3}$ s^{-1}, which is about 2.5 times higher than the rate measured from *in situ* generated catalyst **1**/**L1** ($k = 2.8 \times 10^{-3}$ s^{-1}). Furthermore, to demonstrate its practical utility, a gram-scale reaction was performed for the coupling reaction of acetophenone with 4-methoxybenzylamine by using catalyst **4** (1 mol %), which yielded product **2a** in 90% yield under the standard reaction conditions. These results clearly demonstrate that Ru−catecholate complex **4** is a catalytically relevant species for the alkylation reaction.

DFT Computational Study. While these experimental data showed that the alkylation reaction is an intramolecular process *via* an initially formed imine substrate, we have not been able to detect or trap any catalytically active intermediate species, which makes it very difficult to establish a detailed mechanism of the alkylation step experimentally. We performed density functional theory (DFT) computational analysis to attain deeper insights into the reaction mechanism and to corroborate with the experimental data (Figure 4). To gauge energetics on the alkylation reaction in the absence of a catalyst, we initially carried out the DFT calculations for the sigmatropic transformation of *N*,*N*-ethyl-2-propenylamine (**5**) into pentan-2-imine (**6**) by using a closed-shell M06L/def2-TZVPPD//M06L/def2-SV(P)+PCM(1,4-dioxane) method (Figure 4A). While we have been able to successfully locate the transition state for the [1,3]-sigmatropic shift of ethyl group, the calculated free energy activation value ($\Delta G^{\ddagger}$ = 77.4 kcal/mol) was significantly higher than the total free energy of separated ethyl and amino-isopropenyl radical groups of 62.5 kcal/mol. Moreover, we were unable to find a viable transition state for the sigmatropic transformation by using an open-shell variation of the same computational method, as the calculations led to separate molecular fragments. These initial calculation results clearly suggested that the [1,3]-sigmatropic shift is not a feasible process in the absence of a catalyst.

We next performed the DFT calculations for the alkylation reaction mediated by the Ru−catecholate complex **4**. The calculated structure of complex **4** was modeled from its X-ray crystal structure but without two *t*-Bu groups on the catecholate ligand and used PMe_3 instead of PCy_3 to reduce the computational time (Figure 4B,C). The transformation of **4** into **7a**, which involves the dissociation of one PMe_3 ligand and the coordination of the imine substrate, was calculated to be endothermic of ΔG = 15.3 kcal/mol. We then searched for a energetically viable pathway for the [1,3]-alkyl migration step from **7a** to **8a**. The initial computational efforts to locate the

https://doi.org/10.1021/acscatal.1c04732
ACS Catal. 2021, 11, 13962−13972

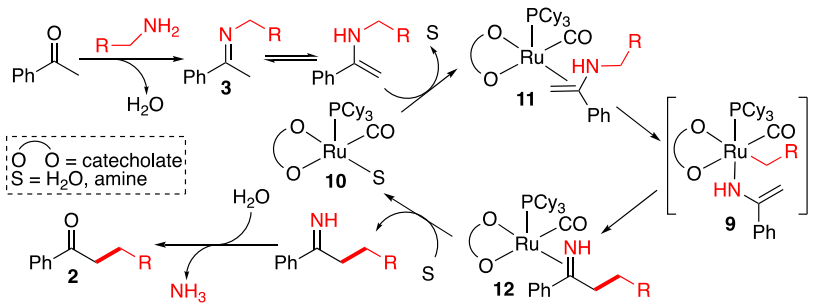

Figure 5. Proposed mechanism of the deaminative α-alkylation of arylketones with amines.

transition state *via* a concerted sigmatropic rearrangement pathway were unsuccessful, despite our numerous attempts by using either closed- or open-shell formalism. The anticipated sigmatropic rearrangement pathway for **7a** to **8a** was eventually found by using the nudged elastic band (NEB) technique at the CASSCF(2,2)/def2-SV(P) level of theory, but the energetically highest point of the pathway was 90 kcal/mol higher than the energy of **7a**, which is prohibitively high for this transformation under normal conditions. Instead, our DFT calculations revealed an alternate stepwise mechanistic pathway *via* the formation of Ru(IV)-alkyl intermediate **9a** (Figure 4B). The geometrically optimized structure of intermediate **9a** showed an octahedral Ru(IV) atom with a covalently bound ethyl moiety. The free energies of activation for both elementary steps were found to be moderate and achievable at 130 °C: $\Delta G^{\ddagger}$ = 42.0 kcal/mol for **7a** → **9a** *via* the transition state **TS-1a**, and $\Delta G^{\ddagger}$ = 22.7 kcal/mol for **9a** → **8a** *via* the transition state **TS-2a**. Recognizing that the activation energy value is still somewhat higher than a typical α-alkylation reaction of ketones, we sought to employ different DFT calculation methods to estimate the energy barrier for the 1,3-alkylation step. For example, single-point calculations by using a BP86 functional method for the steps **7a** → **9a** and **9a** → **8a** resulted in the energy values of $\Delta G^{\ddagger}$ = 34.2 and $\Delta G^{\ddagger}$ = 21.5 kcal/mol, respectively, which are considerably lower than the calculated values from using a M06L functional basis set. While these DFT methods have significant variations in estimating the magnitude of activation energy values, we believe that both DFT calculation methods correctly provided the step-wise [1,3]-alkyl migration step as the most energetically feasible pathway.

The optimized structures of **TS-1a** and **TS-2a** (Figure 4C) represent the migration of the ethyl group from the nitrogen atom to the ruthenium atom and from the ruthenium atom to the terminal carbon atom of the double bond, respectively. The visual analysis of the transition state structures was complemented by the intrinsic reaction coordinate (IRC) analysis that the energy descent along the reaction coordinate from the transition state structure leads to the expected reactants and products. We observed that the reaction proceeds *via* the singlet potential energy surface with a formal Ru(IV) oxidation state, where intermediate **9a** has a partial open-shell character ($\langle S2 \rangle$ = 0.63/0.05 before and after the spin-annihilation procedure, respectively) with a singlet-to-triplet gap of 13.4 kcal/mol.

We next performed the similar calculations for the benzyl-substituted substrate to examine the electronic effects of the imine substrate on the alkylation mechanism. We observed a similar stepwise [1,3]-alkyl migration mechanism that the rearrangement from **7b** to **8b** proceeds *via* the Ru-benzyl intermediate **9b** but with a considerably lower activation energy barrier for the rate-determining step compared to the alkyl-substituted one ($\Delta G^{\ddagger}$ = 32.7 kcal/mol for **7b** → **9b**, $\Delta G^{\ddagger}$ = 21.7 kcal/mol for **9b** → **8b**) (Figure 4B). These computational results are in good agreement with the experimental data in that the aryl-substituted imine substrates lead to the alkylation products at a faster rate than the alkyl-substituted ones. We have also been able to identify the low-energy conformers on the resting state of these complexes by using the conformational search procedure. Taken together, we have successfully computed the entire catalytic cycle for the alkylation reaction, which consists of the initial imine−enamine tautomerization (ΔG = 8.0 kcal/mol), a stepwise 1,3-alkyl migration step **7b** → **9b** ($\Delta G^{\ddagger}$ = 32.7 kcal/mol, ΔG = 12.7 kcal/mol), and the subsequent product formation step **9b** → **8b** ($\Delta G^{\ddagger}$ = 21.7 kcal/mol, ΔG = −27.4 kcal/mol), which is an exothermic step with a relatively low energy barrier. The final step of the catalytic cycle, which involves the substitution of **8** with another imine substrate molecule, is modestly endergonic (ΔG = 7.6 kcal/mol) in forming product **6** and the regeneration of the Ru−catecholate complex **7** (ΔG = 6.6 kcal/mol, Figure S12). As in the case of **7a** to **8a**, the BP86 density functional method predicted a substantially lower activation barrier (7−10 kcal/mol) for the transformation of benzyl-substituted analogue **7b** → **9b** → **8b** compare to the energy values obtained from the M06L functional method. To probe the role of the phosphine ligand on the catalytic activity, we also calculated the energies of Ru-catecholate intermediate species, in which the PMe_3 moiety was replaced by water molecules (Figure S13). The substitution of PMe_3 with water molecules did not dramatically affect the free energy profile, as only a slight increase in the overall activation barrier by 0.8 kcal/mol was obtained comparing to the catalytic cycle based on **4**. On the other hand, the DFT calculations on the Ru catalyst without the catechol moiety resulted in a much higher energy barrier (23 kcal/mol) compared to the Ru catalyst with catecholate ligand **4**, thus highlighting the importance of the catechol ligand in stabilizing these Ru intermediates.

To further validate the DFT calculations on the alkylation mechanism, we computed the carbon KIE for the transformation **7b** → **9b**. Specifically, we evaluated the free energies of **7b** and **TS-1b** for the structures with standard isotopes *versus* the structures with a ^{13}C isotope on the α-carbon atom. We evaluated $\Delta G^{\ddagger}$ for the step **7b** → **9b** based on these free energies and obtained the ratio between the rate constants for the ^{12}C *versus* ^{13}C isotopes on the α-carbon atom by using the Eyring equation. The calculated carbon KIE value (C_{α} = 1.031) was in good agreement with the experimental KIE value (C_{α} = 1.020), which provides a direct support for the stepwise [1,3]-alkyl migration mechanism *via* the formation of Ru-alkyl intermediate **9**.

Proposed Mechanism. We compiled a plausible mechanistic path for the alkylation reaction on the basis of both

https://doi.org/10.1021/acscatal.1c04732
ACS Catal. 2021, 11, 13962−13972

experimental and computational results (Figure 5). The successful synthesis of the Ru−catecholate complex **4** and the demonstration of its high catalytic activity strongly implicate a coordinatively unsaturated Ru(II)−catecholate complex **10** as the catalytically active species. The coordinatively unsaturated Ru−catecholate complex **10** would be generated initially from the treatment of **1** with the reduced form of the benzoquinone ligand *via* the ligand displacement, or directly from **4** *via* PCy_3 ligand dissociation. The dehydrative coupling of ketone and amine substrates and the subsequent imine-to-enamine tautomerization should occur rapidly under the reaction conditions, and the coordination of the enamine form of imine substrate **3** to **10** should form the Ru-enamine species **11**. The reaction profile study showed that the imine **3** is the real substrate for the catalytic alkylation reaction. An extensive H/D exchange to both α- and β-carbon of the ketone product **2a**-*d* from the deuterium labeling study also supports a facile imine-to-enamine tautomerization step.

The first-order kinetics on [**3a**] as well as the lack of imine crossover results provide experimental supports for an intramolecular [1,3]-alkyl migration mechanism in forming the Ru-imine species **12**. The observation of prominent carbon KIE on the α-carbon of product **2a** is also consistent with the C−C bond formation rate-determining step. Although a [1,3]-carbon migration step may occur either in a stepwise or a concerted fashion, we could not find any specific examples of [1,3]-carbon shift on either enamine or imine compounds in the literature. On the other hand, the analogous thermally induced [1,3]-carbon shift reactions of vinylcycloalkanes have been well known to occur in a concerted suprafacial fashion, resulting in the inversion of stereochemistry on the migrating carbon atom.[24] A number of transition-metal-catalyzed C−C coupling reactions of propargylic esters and related cycloisomerization reactions have been known to proceed *via* a [1,3]-carbon shift process,[25] and related Ag-catalyzed [1,3]-halogen shift reactions for vinyl and dienyl-containing compounds have also been reported recently.[26] In these sigmatropic [1,3]-carbon shift reactions, the orbital interactions between the σ-carbon and π-orbitals from unsaturated carbon atoms have been found to be essential for promoting the symmetry-allowed suprafacial carbon migration.

The DFT study revealed new mechanistic insights on the Ru-mediated [1,3]-alkyl migration step of the reaction. The calculations showed that the direct enamine-to-imine rearrangement is a prohibitively high energy process in the absence of a catalyst (Figure 4A). The DFT calculations on the Ru-mediated enamine-to-imine rearrangement showed that the [1,3]-alkyl migration step proceeds in a stepwise fashion *via* the formation of the Ru(IV)-alkyl intermediate species **9**, apparently to avoid a high energy concerted pathway. The geometrical optimization of combining the Ru−catecholate complex **4** with the imine substrate has led to a locally minimized structure of Ru(IV)-alkyl intermediate **9**, with relatively moderate activation free energies ($\Delta G^{\ddagger}$ = 32−42 kcal/mol). Both the DFT computational results as well as experimental Hammett and carbon KIE data clearly indicate that the [1,3]-alkyl migration is the turnover-limiting step of the catalytic reaction, in which the alkyl migration (C−N bond cleavage) step is promoted by nucleophilic α-imine carbon. The rate independence on [H_2O] is consistent with a rapid hydrolysis of the resulting imine product to form alkylation product **2** along with the regeneration of the Ru−catecholate complex **10**. The combined experimental and DFT computational results provided detailed mechanistic insights that the Ru catalytic system (**1**/**L2**) facilitates a normally energetically demanding and previously unexplored deaminative alkylation pathway by promoting an intramolecular stepwise [1,3]-carbon migration process *via* the formation of Ru(IV)-alkyl intermediate species.

CONCLUSIONS

In summary, we have successfully developed a highly regioselective catalytic α-alkylation method of simple ketones from the deaminative coupling with amines. The *in situ*-generated catalytic system consisted of the ruthenium−hydride complex and a redox-active 1,2-benzoquinone ligand (**1**/**L1**) was found to exhibit uniquely high activity and selectivity in promoting the α-alkylation reaction of ketones. Compared to the traditional α-alkylation methods *via* metal-enolates, the catalytic alkylation method offers some sustainable features, in that it is operationally simple, tolerates a variety of common organic functional groups, and does not form any toxic byproducts. Combined experimental and DFT computational studies provided a detailed mechanistic picture for the catalytic alkylation reaction, which comprised the initial formation of the Schiff base from the dehydrative coupling of a ketone with an amine substrate and the imine-to-enamine tautomerization, the Ru-catalyzed turnover-limiting [1,3]-alkyl migration of the enamine substrate, and the imine hydrolysis and substrate−product exchange steps. The DFT study revealed an energetically feasible mechanistic pathway, in which the key step involves a stepwise intramolecular [1,3]-alkyl migration *via* the formation of a Ru(IV)-alkyl species. In light of the successful synthesis of highly active Ru−catecholate complex **4**, we are broadening our search for new catalytic coupling methods that are enabled by transition-metal catalysts having redox-active benzoquinone ligands. We are also systemically probing both electronic as well as redox properties of these catecholate/benzoquinone ligands as a tool for tuning the catalytic activity of Ru complexes.

EXPERIMENTAL SECTION

General Procedure for the Coupling Reaction of a Ketone with an Amine. In a glovebox, complex **1** (3 mol %) and ligand **L1** (10 mol %) were dissolved in 1,4-dioxane (2 mL) in a 25 mL Schlenk tube equipped with a Teflon stopcock and a magnetic stirring bar. The solution was stirred at room temperature for 5 min until the color of solution is turned to a dark reddish brown. After ketone (0.5 mmol) and amine (0.7 mmol) substrates were added to the tube, the tube was brought out of the glovebox, and it was stirred in an oil bath preset at 130 °C for 16 h. The reaction tube was taken out of the oil bath and was cooled to room temperature. After the tube was open to air, the solution was filtered through a short silica gel column by eluting with CH_2Cl_2 (10 mL), and the filtrate was analyzed by GC−MS. An analytically pure product was isolated by column chromatography on silica gel (230−460 mesh, hexanes/EtOAc). The product was completely characterized by NMR and GC−MS spectroscopic methods.

ASSOCIATED CONTENT

Supporting Information

The Supporting Information is available free of charge at https://pubs.acs.org/doi/10.1021/acscatal.1c04732.

Experimental procedures and characterization data for organic products and cartesian coordinates of all computed structures and energy components (PDF)

https://doi.org/10.1021/acscatal.1c04732
ACS Catal. 2021, 11, 13962−13972

X-ray crystallographic data for **2ll** (CIF)
X-ray crystallographic data for **2nn** (CIF)
X-ray crystallographic data for **4** (CIF)

AUTHOR INFORMATION

Corresponding Author

Chae S. Yi − *Department of Chemistry, Marquette University, Milwaukee, Wisconsin 53233, United States;* orcid.org/0000-0002-4504-1151; Email: chae.yi@marquette.edu

Authors

Pandula T. Kirinde Arachchige − *Department of Chemistry, Marquette University, Milwaukee, Wisconsin 53233, United States*

Suhashini Handunneththige − *Department of Chemistry and Biochemistry, New Mexico State University, Las Cruces, New Mexico 88003, United States*

Marat R. Talipov − *Department of Chemistry and Biochemistry, New Mexico State University, Las Cruces, New Mexico 88003, United States;* orcid.org/0000-0002-7559-9666

Nishantha Kalutharage − *Department of Chemistry, Marquette University, Milwaukee, Wisconsin 53233, United States*

Complete contact information is available at: https://pubs.acs.org/10.1021/acscatal.1c04732

Notes

The authors declare no competing financial interest.

ACKNOWLEDGMENTS

Financial support from the National Science of Foundation (CHE-1664652) and the National Institute of Health General Medical Science (R15 GM109273) is gratefully acknowledged. The DFT calculations were performed using computational resources awarded by the Extreme Science and Engineering Discovery Environment (XSEDE) TG-CHE170004. The authors thank Dr. Sergey Lindeman (Marquette University) for X-ray analysis of **2ll**, **2nn**, and **4**.

REFERENCES

(1) (a) Smith, M. B.; March, J. *March's Advanced Organic Chemistry: Reactions, Mechanisms and Structure*, 6th ed.; Wiley-Interscience: New York, 2007. (b) Mukaiyama, T.; Kobayashi, S. Tin(II) Enolates in the Aldol, Michael, and Related Reactions. *Org. React.* **1994**, *46*, 1−103.

(2) Recent reviews: (a) Guillena, G.; Ramón, D. J.; Yus, M. Alcohols as Electrophiles in C-C Bond-Forming Reactions: The Hydrogen Autotransfer Process. *Angew. Chem., Int. Ed.* **2007**, *46*, 2358−2364. (b) Obora, Y. Recent Advances in α-Alkylation Reactions using Alcohols with Hydrogen Borrowing Methodologies. *ACS Catal.* **2014**, *4*, 3972−3981. (c) Chelucci, G. Ruthenium and osmium complexes in C−C bond-forming reactions by borrowing hydrogen catalysis. *Coord. Chem. Rev.* **2017**, *331*, 1−36. (d) Huang, F.; Liu, Z.; Yu, Z. C-Alkylation of Ketones and Related Compounds by Alcohols: Transition-Metal-Catalyzed Dehydrogenation. *Angew. Chem., Int. Ed.* **2016**, *55*, 862−875.

(3) (a) Elangovan, S.; Sortais, J.-B.; Beller, M.; Darcel, C. Iron-Catalyzed α-Alkylation of Ketones with Alcohols. *Angew. Chem., Int. Ed.* **2015**, *54*, 14483−14486. (b) Schlepphorst, C.; Maji, B.; Glorius, F. Ruthenium-NHC Catalyzed α-Alkylation of Methylene Ketones Provides Branched Products through Borrowing Hydrogen Strategy. *ACS Catal.* **2016**, *6*, 4184−4188. (c) Zhang, G.; Wu, J.; Zeng, H.; Zhang, S.; Yin, Z.; Zheng, S. Cobalt-Catalyzed α-Alkylation of Ketones with Primary Alcohols. *Org. Lett.* **2017**, *19*, 1080−1083. (d) Akhtar, W. M.; Cheong, C. B.; Frost, J. R.; Christensen, K. E.; Stevenson, N. G.; Donohoe, T. J. Hydrogen Borrowing Catalysis with Secondary Alcohols: A New Route for the Generation of β-Branched Carbonyl Compounds. *J. Am. Chem. Soc.* **2017**, *139*, 2577−2580. (e) Chakraborty, S.; Daw, P.; David, Y. B.; Milstein, D. Manganese-Catalyzed α-Alkylation of Ketones, Esters, and Amides Using Alcohols. *ACS Catal.* **2018**, *8*, 10300−10305. (f) Gawali, S. S.; Pandia, B. K.; Pal, S.; Gunanathan, C. Manganese(I)-Catalyzed Cross-Coupling of Ketones and Secondary Alcohols with Primary Alcohols. *ACS Omega* **2019**, *4*, 10741−10754. (g) Das, J.; Vellakkaran, M.; Banerjee, D. Nickel-Catalyzed Alkylation of Ketone Enolates: Synthesis of Monoselective Linear Ketones. *J. Org. Chem.* **2019**, *84*, 769−779.

(4) Huang, Z.; Lim, H. N.; Mo, F.; Young, M. C.; Dong, G. Transition metal-catalyzed ketone-directed or mediated C-H functionalization. *Chem. Soc. Rev.* **2015**, *44*, 7764−7786.

(5) (a) Pirnot, M. T.; Rankic, D. A.; Martin, D. B. C.; MacMillan, D. W. C. Photoredox Activation for the Direct -Arylation of Ketones and Aldehydes. *Science* **2013**, *339*, 1593−1596. (b) Petronijević, F. R.; Nappi, M.; MacMillan, D. W. C. Direct β-Functionalization of Cyclic Ketones with Aryl Ketones via the Merger of Photoredox and Organocatalysis. *J. Am. Chem. Soc.* **2013**, *135*, 18323−18326.

(6) Okada, M.; Fukuyama, T.; Yamada, K.; Ryu, I.; Ravelli, D.; Fagnoni, M. Sunlight photocatalyzed regioselective β-alkylation and acylation of cyclopentanones. *Chem. Sci.* **2014**, *5*, 2893−2898.

(7) (a) Wang, X.; Pei, T.; Han, X.; Widenhoefer, R. A. Palladium-Catalyzed Intramolecular Hydroalkylation of Unactivated Olefins with Dialkyl Ketones. *Org. Lett.* **2003**, *5*, 2699−2701. (b) Qian, H.; Pei, T.; Widenhoefer, R. A. Development, Scope, and Mechanism of the Palladium-Catalyzed Intramolecular Hydroalkylation of 3-Butenyl β-Diketones. *Organometallics* **2005**, *24*, 287−301. (c) Xiao, Y.-P.; Liu, X.-Y.; Che, C.-M. Efficient Gold(I)-Catalyzed Direct Intramolecular Hydroalkylation of Unactivated Alkenes with α-Ketones. *Angew. Chem., Int. Ed.* **2011**, *50*, 4937−4941.

(8) (a) Mo, F.; Dong, G. Regioselective ketone α-alkylation with simple olefins via dual activation. *Science* **2014**, *345*, 68−72. (b) Xing, D.; Dong, G. Branched-Selective Intermolecular Ketone α-Alkylation with Unactivated Alkenes via an Enamide Directing Strategy. *J. Am. Chem. Soc.* **2017**, *139*, 13664−13667.

(9) Ouyang, K.; Hao, W.; Zhang, W.-X.; Xi, Z. Transition-Metal-Catalyzed Cleavage of C-N Single Bonds. *Chem. Rev.* **2015**, *115*, 12045−12090.

(10) Klauck, F. J. R.; James, M. J.; Glorius, F. Deaminative Strategy for the Visible-Light-Mediated Generation of Alkyl Radicals. *Angew. Chem., Int. Ed.* **2017**, *56*, 12336−12339.

(11) Zhao, X.; Liu, D.; Guo, H.; Liu, Y.; Zhang, W. C-N Bond Cleavage of Allylic Amines via Hydrogen Bond Activation with Alcohol Solvents in Pd-Catalyzed Allylic Alkylation of Carbonyl Compounds. *J. Am. Chem. Soc.* **2011**, *133*, 19354−19357.

(12) Sun, S.-Z.; Romano, C.; Martin, R. Site-Selective Catalytic Deaminative Alkylation of Unactivated Olefins. *J. Am. Chem. Soc.* **2019**, *141*, 16197−16201.

(13) Fu, M.-C.; Shang, R.; Zhao, B.; Wang, B.; Fu, Y. Photocatalytic decarboxylative alkylations mediated by triphenylphosphine and sodium iodide. *Science* **2019**, *363*, 1429−1434.

(14) Recent Reviews: (a) Wang, Q.; Su, Y.; Li, L.; Huang, H. Transition-metal catalysed C-N bond activation. *Chem. Soc. Rev.* **2016**, *45*, 1257−1272. (b) Dander, J. E.; Garg, N. K. Breaking Amides Using Nickel Catalysis. *ACS Catal.* **2017**, *7*, 1413−1423.

(15) Kalutharage, N.; Yi, C. S. Deaminative and Decarboxylative Catalytic Alkylation of Amino Acids with Ketones. *Angew. Chem., Int. Ed.* **2013**, *52*, 13651−13655.

(16) (a) Arachchige, P. T. K.; Lee, H.; Yi, C. S. Synthesis of Symmetric and Unsymmetric Secondary Amines from the Ligand-Promoted Ruthenium-Catalyzed Deaminative Coupling Reaction of Primary Amines. *J. Org. Chem.* **2018**, *83*, 4932−4947. (b) Arachchige, P. T. K.; Yi, C. S. Synthesis of Quinazoline and Quinazolinone Derivatives via Ligand-Promoted Ruthenium-Catalyzed Dehydrogenative and Deaminative Coupling Reaction of 2-Aminophenyl Ketones and 2-Aminobenzamides with Amines. *Org. Lett.* **2019**, *21*, 3337−3341.

(17) (a) He, J.; Wasa, M.; Chan, K. S. L.; Shao, Q.; Yu, J.-Q. Palladium-Catalyzed Transformations of Alkyl C-H Bonds. *Chem. Rev.* **2017**, *117*, 8754−8786. (b) Rej, S.; Chatani, N. Rhodium-Catalyzed

C(sp^2)- or C(sp^3)−H Bond Functionalization Assisted by Removable Directing Groups. *Angew. Chem., Int. Ed.* **2019**, *58*, 8304−8329.

(18) (a) Ritleng, V.; Sirlin, C.; Pfeffer, M. Ru-, Rh-, and Pd-Catalyzed C−C Bond Formation Involving C−H Activation and Addition on Unsaturated Substrates: Reactions and Mechanistic Aspects. *Chem. Rev.* **2002**, *102*, 1731−1770. (b) Kakiuchi, F.; Kochi, T.; Mizushima, E.; Murai, S. Room-Temperature Regioselective C−H/Olefin Coupling of Aromatic Ketones Using an Activated Ruthenium Catalyst with a Carbonyl Ligand and Structural Elucidation of Key Intermediates. *J. Am. Chem. Soc.* **2010**, *132*, 17741−17750.

(19) Recent selected examples: (a) Matsubara, R.; Kobayashi, S. Enamides and Enecarbamates as Nucleophiles in Stereoselective C-C and C-N Bond-Forming Reactions. *Acc. Chem. Res.* **2008**, *41*, 292−301. (b) Kovács, G.; Lledós, A.; Ujaque, G. Hydroamination of Alkynes with Ammonia: Unforeseen Role of the Gold(I) Catalyst. *Angew. Chem., Int. Ed.* **2011**, *50*, 11147−11151. (c) Li, L.; Liu, P.; Su, Y.; Huang, H. Palladium-Catalyzed Aminomethylamination and Aromatization of Aminoalkenes with Aminals via C-N Bond Activation. *Org. Lett.* **2016**, *18*, 5736−5739. (d) Fang, G.; Liu, J.; Fu, J.; Liu, Q.; Bi, X. Silver-Catalyzed Cascade Reaction of β-Enaminones and Isocyanoacetates To Construct Functionalized Pyrroles. *Org. Lett.* **2017**, *19*, 1346−1349. (e) Jin, M.; Yin, S.-f.; Yang, S.-D. Bismuth(III)-Catalyzed Sequential Enamine-Imine Tautomerism/2-Aza-Cope Rearrangement of Stable β-Enaminophosphonates: One-Pot Synthesis of β-Aminophosphonates. *Org. Lett.* **2020**, *22*, 2811−2815.

(20) A reviewer pointed out that the Hammett data could have been influenced from the initial imine formation rather than from the subsequent formation of the alkylation products. To address the reviewer's concerns, we repeated the Hammett correlation experiment by using the *para*-substituted imines **3**, which showed an identical trend as the one shown in Figure 2.

(21) (a) Singleton, D. A.; Thomas, A. A. High-Precision Simultaneous Determination of Multiple Small Kinetic Isotope Effects at Natural Abundance. *J. Am. Chem. Soc.* **1995**, *117*, 9357−9358. (b) Frantz, D. E.; Singleton, D. A.; Snyder, J. P. ^{13}C Kinetic Isotope Effects for the Addition of Lithium Dibutylcuprate to Cyclohexenone. Reductive Elimination Is Rate-Determining. *J. Am. Chem. Soc.* **1997**, *119*, 3383−3384. (c) Nowlan, D. T.; Gregg, T. M.; Davies, H. M. L.; Singleton, D. A. Isotope Effects and the Nature of Selectivity in Rhodium-Catalyzed Cyclopropanations. *J. Am. Chem. Soc.* **2003**, *125*, 15902−15911.

(22) (a) Frantz, D. E.; Singleton, D. A. Isotope Effects and the Mechanism of Chlorotrimethylsilane-Mediated Addition of Cuprates to Enones. *J. Am. Chem. Soc.* **2000**, *122*, 3288−3295. (b) Singleton, D. A.; Wang, Z. Isotope Effects and the Nature of Enantioselectivity in the Shi Epoxidation. The Importance of Asynchronicity. *J. Am. Chem. Soc.* **2005**, *127*, 6679−6685. (c) Hirschi, J. S.; Takeya, T.; Hang, C.; Singleton, D. A. Transition-State Geometry Measurements from ^{13}C Isotope Effects. The Experimental Transition State for the Epoxidation of Alkenes with Oxaziridines. *J. Am. Chem. Soc.* **2009**, *131*, 2397−2403.

(23) The analogous reaction of **1** with the benzoquinone ligand **L1** formed a mixture of products, and we were not able to separate the complex **4** from the mixture.

(24) (a) Leber, P. A.; Baldwin, J. E. Thermal [1,3] Carbon Sigmatropic Rearrangements of Vinylcyclobutanes. *Acc. Chem. Res.* **2002**, *35*, 279−287. (b) Baldwin, J. E.; Leber, P. A. Molecular rearrangements through thermal [1,3] carbon shifts. *Org. Biomol. Chem.* **2008**, *6*, 36−47.

(25) (a) Marion, N.; Nolan, S. P. Propargylic Esters in Gold Catalysis: Access to Diversity. *Angew. Chem., Int. Ed.* **2007**, *46*, 2750−2752. (b) Rao, W.; Susanti, D.; Chan, P. W. H. Gold-Catalyzed Tandem 1,3-Migration/[2 + 2] Cycloaddition of 1,7-Enyne Benzoates to Azabicyclo[4.2.0]oct-5-enes. *J. Am. Chem. Soc.* **2011**, *133*, 15248−15251. (c) Chen, C.; Zou, Y.; Chen, X.; Zhang, X.; Rao, W.; Chan, P. W. H. Gold-Catalyzed Tandem 1,3-Migration/Double Cyclopropanation of 1-Ene-4,*n*-diyne Esters to Tetracyclodecene and Tetracycloundecene Derivatives. *Org. Lett.* **2016**, *18*, 4730−4733. (d) Ren, Y.; Lin, Z. Theoretical Studies on Rh-Catalyzed Cycloisomerization of Homopropargylallene-Alkynes through C(sp^3)-C(sp) Bond Activation. *ACS Catal.* **2020**, *10*, 1828−1837.

(26) (a) Grigg, R. D.; van Hoveln, R.; Schomaker, J. M. Copper-Catalyzed Recycling of Halogen Activating Groups via 1,3-Halogen Migration. *J. Am. Chem. Soc.* **2012**, *134*, 16131−16134. (b) Shiroodi, R. K.; Dudnik, A. S.; Gevorgyan, V. Stereocontrolled 1,3-Phosphatyloxy and 1,3-Halogen Migration Relay toward Highly Functionalized 1,3-Dienes. *J. Am. Chem. Soc.* **2012**, *134*, 6928−6931. (c) van Hoveln, R. J.; Schmid, S. C.; Tretbar, M.; Buttke, C. T.; Schomaker, J. M. Formal asymmetric hydrobromination of styrenes *via* copper-catalyzed 1,3-halogen migration. *Chem. Sci.* **2014**, *5*, 4763−4767. (d) van Hoveln, R.; Hudson, B. M.; Wedler, H. B.; Bates, D. M.; Le Gros, G.; Tantillo, D. J.; Schomaker, J. M. Mechanistic Studies of Copper(I)-Catalyzed 1,3-Halogen Migration. *J. Am. Chem. Soc.* **2015**, *137*, 5346−5354.

https://doi.org/10.1021/acscatal.1c04732
ACS Catal. 2021, 11, 13962−13972